

Rescuing Quadratic Inflation

John Ellis, Malcolm Fairbairn and Maria Sueiro

Theoretical Particle Physics and Cosmology Group,
Physics Department, King's College London,
Strand, London WC2R 2LS, UK

Abstract

Inflationary models based on a single scalar field ϕ with a quadratic potential $V = \frac{1}{2}m^2\phi^2$ are disfavoured by the recent Planck constraints on the scalar index, n_s , and the tensor-to-scalar ratio for cosmological density perturbations, r_T . In this paper we study how such a quadratic inflationary model can be rescued by postulating additional fields with quadratic potentials, such as might occur in sneutrino models, which might serve as either curvatons or supplementary inflatons. Introducing a second scalar field reduces but does not remove the pressure on quadratic inflation, but we find a sample of three-field models that are highly compatible with the Planck data on n_s and r_T . We exhibit a specific three-sneutrino example that is also compatible with the data on neutrino mass difference and mixing angles.

KCL-PH-TH/2013-40, LCTS/2013-27, CERN-PH-TH/2013-293

1 Introduction

Inflation is a very promising paradigm for the behaviour of the scale factor in the early Universe, which offers a solution to the cosmological horizon problem, explaining the observed large-scale isotropy and giving rise to small fluctuations in energy density as observed in the cosmic microwave background (CMB) radiation that seeded galactic structure formation, as well as explaining the absence of topological defects. In the simplest models of inflation, the energy density responsible for the accelerated early expansion of the scale factor arises from the expectation value of a scalar field rolling down a potential. As discussed in [1], a huge number of candidate scalar fields appearing in extensions of the standard model of particle physics and in models with modified gravitational sectors have the freedom to match observations: for a sampling of recent models, see [2, 3, 4, 5, 6, 7, 8, 9, 10, 11, 12].

In the simplest class of single-field models, the energy density in the potential causes an accelerated expansion of the Universe, with the strength of tensor perturbations being directly related to the magnitude of the energy density. Since the inflaton ϕ rolls slowly down the potential, the spectrum of scalar perturbations is tilted. Once the value of ϕ

becomes sub-Planckian, the slow roll ends and the field starts to oscillate and then decays into radiation, reheating the Universe. This simplest model makes surprisingly successful predictions for the main inflationary observables. For example, it provides an almost scale-invariant spectrum of density perturbations and predicts that the non-Gaussianity parameter f_{NL} is relatively small.

The simplest scenario is a single scalar field ϕ with a monomial potential such as $\frac{1}{2}m^2\phi^2$ or $\lambda\phi^4$. However, $\lambda\phi^4$ models were already under pressure from the results of WMAP [13] and can now be regarded as excluded by the observations of the Planck satellite [14, 15], and quadratic $\frac{1}{2}m^2\phi^2$ models are now also under severe pressure, since they are unable to fit simultaneously the observed spectral index of scalar perturbations n_s and the low tensor-to-scalar ratio r_T .

For a range of typical values of the number of efolds during inflation, $N_* \in [40, 60]$, single-field inflationary models with a $\frac{1}{2}m^2\phi^2$ potential predict a value for r_T in the range $[0.1, 0.2]$, whereas the Planck data require $r_T < 0.1$. For a lower value of N_* , i.e., a smaller amount of expansion between the largest scales leaving the horizon and the end of inflation, it is possible for a quadratic model to give a value for r_T that obeys the Planck constraint, but the quadratic model then makes a prediction for the spectral index of the perturbations n_s that does not respect the Planck constraint $n_s = 0.9624 \pm 0.0075$, since there is a one-to-one mapping between the number of efolds and the scalar spectral index.

In this work we explore ways to rescue models with quadratic potentials. Our objective is to find a model of quadratic inflation that (i) gives the correct magnitude for the scalar density perturbation δ , (ii) yields a Planck-compatible value of the scalar spectral index n_s , (iii) predicts a value for the tensor-to-scalar ratio r_T that obeys the Planck constraint, and (iv) does not predict significant non-Gaussianity.

Attaining all these objectives simultaneously requires modifying the mapping between the number of efolds and the scalar spectral index. This may be done by introducing extra fields that act either as secondary inflatons or as curvatons. We restrict our attention to minimal models with multiple $\frac{1}{2}m^2\phi^2$ potentials. Apart from simplicity, one of our motivations for this restriction is the idea that the inflaton might be a singlet sneutrino in a supersymmetric seesaw model of neutrino masses [16], which is a motivated and minimal extension of the Standard Model. In such a scenario, there must be at least two such sneutrino fields so that two light neutrinos can acquire masses, and probably three so that all three light neutrinos can be massive.

In the next Section we review the simplest case of a single $\frac{1}{2}m^2\phi^2$ inflationary field, and the above-mentioned reasons why it has difficulties fitting the latest data. In Section 3 we go on to examine models with an additional scalar field acting as a curvaton. Whilst the disagreement with the data can be reduced in such scenarios, they are still in some tension with the data, although not enough to be considered as excluded. Then, in Section 4 we look at models with two inflatons acting in consort accompanied by an curvaton, which we find to be the minimal combination of quadratic fields that obeys completely all the Planck constraints. In Section 5 we show how such a supersymmetric seesaw model can be realized with the three quadratic scalar fields being interpreted as supersymmetric partners of heavy singlet neutrinos, showing how such a model can fit simultaneously the available data on neutrino oscillations. Finally, Section 6 contains a summary and discusses future prospects for quadratic inflationary models.

2 Single-Field Quadratic Inflation

We first review the standard lore for single-field inflation with a quadratic potential $V = \frac{1}{2}m_\phi^2\phi^2$. The power spectrum of the scalar perturbations is given by [17, 18]

$$\mathcal{P}_\zeta = \left(\frac{H_*}{\dot{\phi}_*}\right)^2 \left(\frac{H_*}{2\pi}\right)^2 = \frac{\phi_*^2}{4M_{Pl}^4} \left(\frac{H_*}{2\pi}\right)^2, \quad (1)$$

where starred quantities correspond to the values of the various parameters at the epoch at which the last scales to re-enter the horizon before the last scattering surface were initially leaving the horizon during inflation. The Hubble parameter is given by the Friedmann equation $H^2 = V/(3M_{Pl}^2)$, where M_{Pl} is the reduced Planck mass, $M_{Pl} = (8\pi G)^{-1/2} = 2.4 \times 10^{18}$ GeV. The density perturbation is $\delta_H^2 \equiv \frac{4}{25}\mathcal{P}_\zeta$ [17], so using the above equation we have

$$\delta_H = \sqrt{\frac{1}{600\pi^2} \frac{m_\phi \phi_*^2}{M_{Pl}^3}}. \quad (2)$$

The two slow-roll parameters in this case are:

$$\epsilon \equiv \frac{M_{Pl}^2}{2} \left(\frac{V'}{V}\right)^2 = \frac{2M_{Pl}^2}{\phi^2} \quad ; \quad \eta \equiv M_{Pl}^2 \frac{V''}{V} = \frac{2M_{Pl}^2}{\phi^2}, \quad (3)$$

where dashed quantities denote derivatives with respect to ϕ .

The scalar spectral index is given in terms of the slow-roll parameters by $n_s - 1 = -6\epsilon_* + 2\eta_*$ [19], so in this case it is given by

$$n_s - 1 = -\frac{8M_{Pl}^2}{\phi_*^2}. \quad (4)$$

The tensor-to-scalar ratio r_T is defined as the ratio of the power spectrum of the tensor perturbations [20]

$$\mathcal{P}_T = \frac{8}{M_{Pl}^2} \left(\frac{H_*}{2\pi}\right)^2 \quad (5)$$

to the power spectrum of the scalar perturbations, given in (1). In the simple quadratic inflation model the tensor-to-scalar ratio is given by

$$r_T \equiv \frac{\mathcal{P}_T}{\mathcal{P}_\zeta} = \frac{32M_{Pl}^2}{\phi_*^2}, \quad (6)$$

yielding a very restrictive relationship between the tensor-to-scalar ratio and the scalar spectral index:

$$r_T = 4(1 - n_s). \quad (7)$$

Ultimately, both quantities are fixed by the expectation value of the inflaton corresponding to the scales entering the horizon at the last scattering surface, which is around 40-60 efolds before the end of inflation. In a particular model the exact number of efolds is not a free parameter, but depends upon the rate at which the coherent oscillations of the inflaton decay into radiation after inflation.

m_ϕ	Γ_ϕ
----------	---------------

Free parameters for single-field quadratic inflation.

m_ϕ	Γ_ϕ	m_σ	Γ_σ	σ_*
----------	---------------	------------	-----------------	------------

Free parameters for the model with a quadratic inflaton and a quadratic curvaton.

m_ϕ	m_χ	Γ_χ	$\theta_{\phi\chi*}$	m_σ	Γ_σ	σ_*
----------	----------	---------------	----------------------	------------	-----------------	------------

Free parameters for the model with two quadratic inflatons and a quadratic curvaton.

Table 1: Free parameters in the quadratic inflation models discussed in the text.

To find the time t_* when the largest scale crosses the horizon during inflation, we must solve the equation

$$N_* = 60 - \ln \frac{10^{16} \text{ GeV}}{V_*^{1/4}} + \ln \frac{V_*^{1/4}}{V_{end}^{1/4}} - \frac{1}{3} \ln \frac{V_{end}^{1/4}}{\rho_{\text{last decay}}^{1/4}}, \quad (8)$$

where V_{end} is the potential at the end of inflation and $\rho_{\text{last decay}}$ is the energy density evaluated at the time of the decay of the longest-lived field in the theory [17]. Solving (8) is quite simple for quadratic inflation, and means that the number of efolds N_* , and therefore the time of horizon crossing t_* , is not an arbitrary parameter but is constrained for a given set of masses and decay rates. A change in the duration of matter or radiation domination of the energy density up until the last decay when the Universe is thermalized for the last time will affect the value of N_* . In the case of single-field ϕ^2 (quadratic) inflation, the two model parameters are therefore the inflaton mass m_ϕ and its decay rate Γ_ϕ , as shown in the first row of Table 1.

The rigid relationship (7) between n_s and r_T is plotted in Fig. 1, where it can be seen that single-field ϕ^2 (quadratic) inflation does not fit the data very well, no matter what the number of efolds.

3 Model with one Inflaton and one Curvaton

We now consider a second model that contains, in addition to the field ϕ with a quadratic potential that acts as the inflaton, a second scalar field with a quadratic potential that acts as the curvaton σ [21]. This model is therefore described by

$$V = \frac{1}{2}m_\phi^2\phi^2 + \frac{1}{2}m_\sigma^2\sigma^2. \quad (9)$$

The curvaton field σ is frozen at an expectation value σ_* during the slow-roll of ϕ since $H \gg m_\sigma$. After inflation ends and the Hubble parameter becomes comparable to the curvaton mass, $H \sim m_\sigma$, the curvaton begins to oscillate around the minimum of its potential. When the Hubble parameter falls to the curvaton decay rate, Γ_σ , the curvaton decays to radiation. The parameters of this model are the masses and decay rates of the inflaton and the curvaton, m_ϕ , Γ_ϕ and m_σ , Γ_σ respectively, and the expectation value of the curvaton during inflation σ_* , as listed in the second row of Table 1.

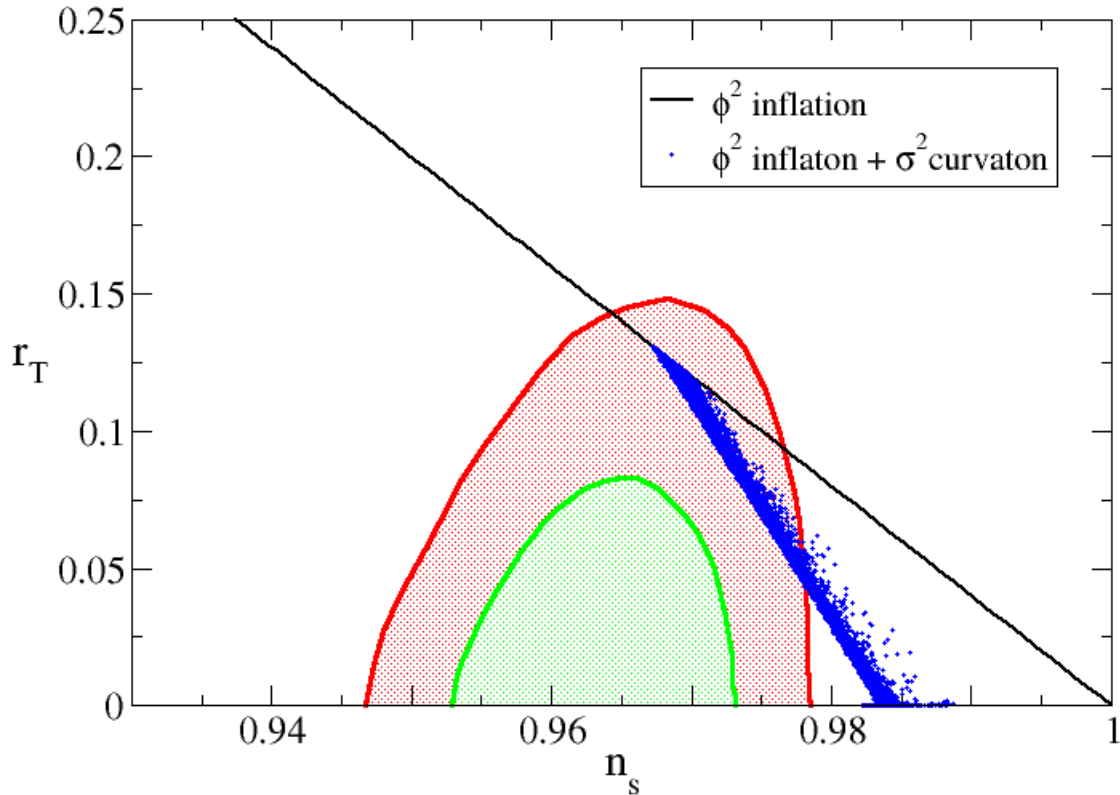


Figure 1: The plane of the spectral index n_s and the tensor-to-scalar ratio r_T . The shaded regions correspond to the 1- and 2- σ constraints obtained by combining Planck and baryon acoustic oscillation (BAO) data [15]. The single black line corresponds to minimal ϕ^2 (quadratic) inflation, and the blue points are combinations of a ϕ^2 inflaton and a σ^2 (quadratic) curvaton, which reduces to ϕ^2 inflation as a limiting case when the curvaton corrections are negligible.

Now, although only ϕ is responsible for providing the expansion of the Universe during inflation, both fields can contribute to δ_H , n_s , and r_T . From [22, 23] we see that the total density perturbation is given by

$$\delta_H = \delta_{H\phi} + \frac{f_\sigma}{3} \delta_{H\sigma}, \quad (10)$$

with the individual components evaluated at horizon crossing ¹, where we have

$$\delta_{H\phi} = \sqrt{\frac{1}{600\pi^2} \frac{m_\phi \phi_*^2}{M_{Pl}^3}} \quad ; \quad \delta_{H\sigma} = \left(\frac{H_*}{\pi \sigma_*} \right), \quad (11)$$

and f_σ is evaluated at the epoch of the last decay, i.e., the epoch at which the curvaton decays, rather than the inflaton, so that

$$f_\sigma = \left(\frac{3\Omega_\sigma}{4 - \Omega_\sigma} \right)_{\text{last decay}}, \quad (12)$$

where $\Omega_\sigma = \rho_\sigma / \rho_{tot}$ at the epoch of curvaton decay [24, 25, 26]. The power spectrum of the created density perturbation is then

$$\mathcal{P}_\zeta \propto \delta_{H\phi}^2 + \frac{f_\sigma^2}{9} \delta_{H\sigma}^2, \quad (13)$$

and to evaluate the spectral index we simply use the definition

$$n_s - 1 \equiv \frac{d \ln \mathcal{P}}{d \ln k} = \frac{\sqrt{3} M_{Pl}}{\sqrt{V_*} \mathcal{P}} \frac{d \mathcal{P}}{dt}, \quad (14)$$

where we transformed the derivative using $d \ln k = H dt$, and note that the expansion H is dominated by the effects of V at this epoch, which is during slow-roll inflation. The tensor-to-scalar ratio is

$$r_T \equiv \frac{\mathcal{P}_T}{\mathcal{P}_\zeta}, \quad (15)$$

which may be evaluated using (13) and

$$\mathcal{P}_T = \frac{2V_*}{3\pi^2 M_{Pl}^4}. \quad (16)$$

Once the time t_* has been established in the same way as in Section 2, we can calculate the density perturbation using (10), the spectral index using (14), and the tensor-to-scalar ratio using (15). Employing a Markov Chain Monte Carlo algorithm, we fit the measured values of δ_H and n_s and explore the predictions for r_T , as shown in Figs. 1 and 2.

We find in our sampling of its five-parameter space that this model is able to predict a low value for the tensor-to-scalar ratio r_T , well under the constraint coming from Planck. This happens when the curvaton field is significant at the time of the last decay, and dominates the energy density. However, obtaining a low value for r_T is possible only at the expense of an unsuccessful prediction for the scalar spectral index. As is shown in the left panel of Fig.

¹All quantities evaluated at this time have the index *.

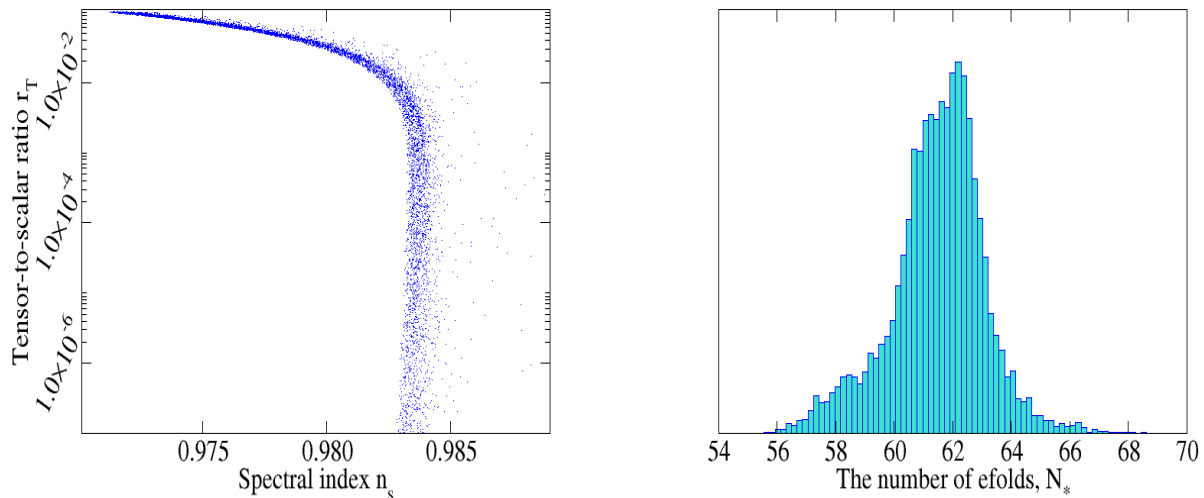


Figure 2: The left panel shows the spectral index n_s and the tensor-to-scalar ratio r_T in the model with one inflaton and one curvaton (same data as figure 1 but on log scale). Here, we show only the points that have a value for r_T that is lower than the Planck constraint of $r_T < 0.1$. This occurs only for values of n_s that are significantly larger than that measured. In the right panel, we show the values of the number of e-folds N_* in this model, which is in the range $[55, 70]$.

(2), when r_T falls to a value below 0.1, n_s grows to a value that is approximately 3σ away from the current measurement as $r_T \rightarrow 0$.

This conclusion differs from the results in [25], where a Planck-consistent value of r_T was found in a fit to the values of δ_H and n_s in a model with one inflaton and one curvaton. The reason for this difference is that in [25] the inflationary scale at horizon crossing was set by hand by assuming $\epsilon_* = 0.02$, which corresponds to a very low number of e-folds, $N_* \sim 25$. In contrast, in our work we solve for the field value at t_* , so that our model is self-consistent. We find that N_* has to be in the range $[55, 70]$ as shown in the right plot of Fig. (2).

We find that the values of r_T and n_s depend strongly on the value of the inflaton mass, m_ϕ . As is shown in the left panel of Fig. 3, a lower value of r_T can be obtained with a lower value of m_ϕ , but this corresponds to a higher value of n_s . This behaviour is seen also in Fig. 1, where one can see that, although curvaton models fit the Planck data somewhat better than single-field quadratic inflation, they are still disfavoured, as they do not come within the 68% CL region favoured by the Planck + BAO data.

We therefore conclude that, although a model with one inflaton and one curvaton, with both fields contributing to the generation of the perturbations, is able to predict a value for r_T that is within the Planck constraint, this model cannot combine this good prediction with a successful prediction for the spectral index n_s .

This conclusion could be relaxed by assuming additional inflation at some later time in the Universe as in, e.g., thermal inflation [17, 20]. However, it seems quite difficult to obtain enough thermal inflation to reconcile the Planck data on r_T and n_s with the model combining a quadratic inflaton and a quadratic curvaton, since typically one requires 25-30 e-folds of

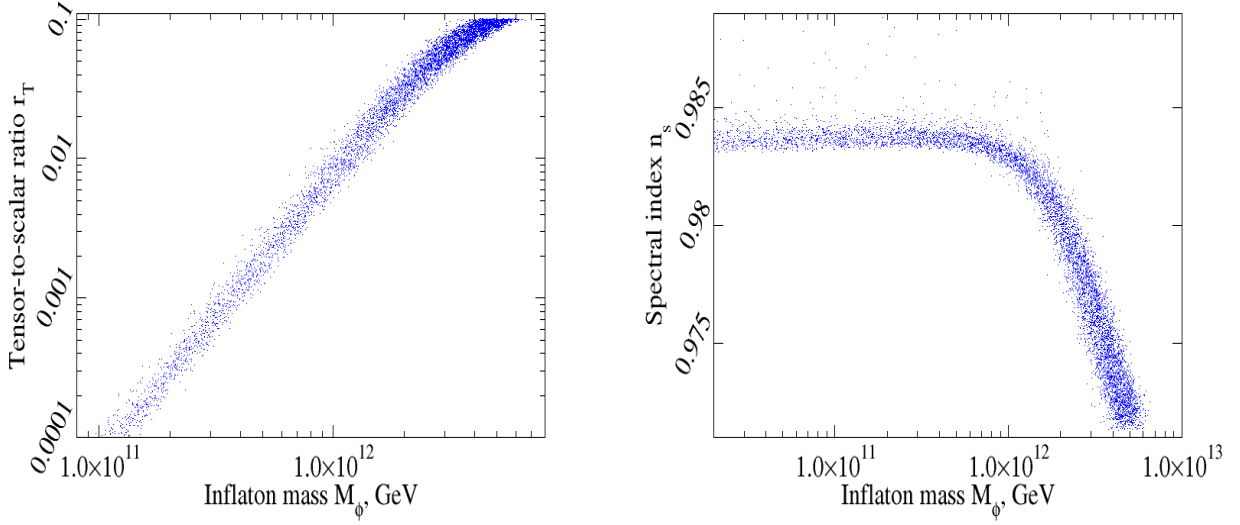


Figure 3: *The left panel shows the dependence of the tensor-to-scalar ratio r_T on the inflaton mass m_ϕ . We see that obtaining a lower value for r_T , so as to be consistent with the constraint coming from Planck, would require a lower inflaton mass. However, as is shown in the right panel, lower values of m_ϕ result in values of n_s that are significantly higher than the measured one.*

later inflation.

4 Model with two Inflavons and one Curvaton

In view of this setback, in this Section we further augment the model by including another scalar field, χ . This is assumed to be a second inflaton field, again with a quadratic term in the potential, so that it becomes

$$V = \frac{1}{2}m_\phi^2\phi^2 + \frac{1}{2}m_\chi^2\chi^2 + \frac{1}{2}m_\sigma^2\sigma^2. \quad (17)$$

In this case, both ϕ and χ roll slowly down their potentials, giving rise to inflation while, as before, the curvaton field σ remains frozen at its expectation value during inflation and then oscillates and decays into radiation.

Curvaton domination of the energy density in this model can lead to a low value of r_T consistent with the Planck data, while the addition of the second inflaton helps to lower the prediction for n_s , making the model consistent with the Planck value. This is because, in the case of curvaton dominance, the power spectrum of the scalar density perturbations is simply $P_\zeta = (H_*/(\pi\sigma_*))^2$. Then, from the expression (14) for the spectral index we obtain the expression:

$$n_\sigma = \frac{\sqrt{3}M_{Pl}}{V_*^{3/2}} \frac{dV_*}{dt} + 1. \quad (18)$$

We see from (18) that, in order to alter the high value of n_s that was obtained in the two-field (ϕ, σ) model we must alter the time derivative of the potential evaluated at horizon crossing.

Since the curvaton expectation value does not change during inflation, it is only with the addition of the second inflaton χ that we can achieve this.

Substituting (17) in (18), we obtain the following expression for the scalar spectral index in terms of our model parameters:

$$n_\sigma - 1 = \frac{-M_{Pl}^2 m_\phi^4 \phi_*^2}{V_*^2} \left(1 + \left(\frac{m_\chi}{m_\phi} \right)^4 \left(\frac{\chi_*}{\phi_*} \right)^2 \right). \quad (19)$$

In our numerical analysis, we find that the heavier of the two inflaton fields (let us call it ϕ) stops rolling once its expectation value drops down to the Planck scale. It then begins to oscillate, but the Universe is still expanding exponentially due to the other inflaton field. This means that ϕ is redshifted, with its expectation value dropping rapidly, and by the end of inflation, i.e., when the expectation value of χ becomes equal to M_{Pl} , the contribution of ϕ to the energy density is negligible. It is therefore not necessary to include the decay rate of the heavy inflaton among the relevant parameters of our model listed in the third row of Table 1. The parameter $\theta_{\phi\chi*} \equiv \tan^{-1}(\chi_*/\phi_*)$ corresponds to the angle in field space at t_* , i.e. the angle between the ϕ and χ direction when the largest scales in the CMB are leaving the horizon. Typically the lighter field χ will be frozen at this moment, although we do not assume this, since we analyze this stage numerically.

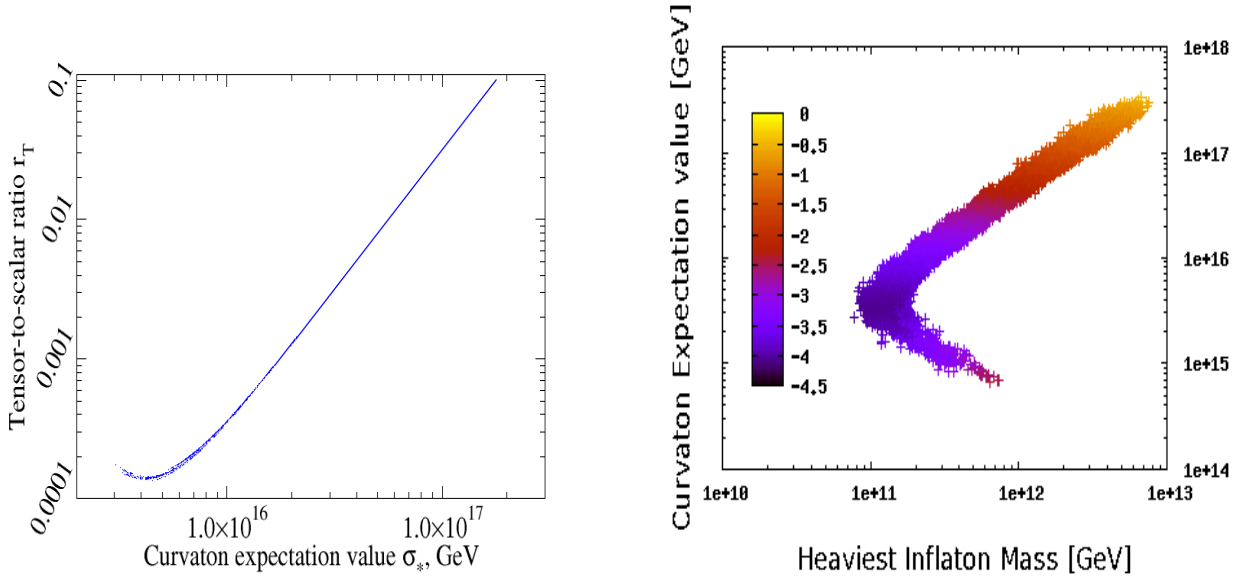


Figure 4: The left panel shows the strong dependence of r_T on the curvaton expectation value σ_* in the model with two inflatons and one curvaton with quadratic potentials. In the right panel we plot the mass of the heaviest inflaton vs. the curvaton expectation value. The colours denote ranges of $\log_{10}(r_T)$. In both plots the turn in the curve separates curvaton behaviour from pure inflationary behaviour in which the curvaton energy density always remains small.

As in the model with one inflaton and one curvaton, we solve equation (8) numerically to find the time during inflation when the largest scales left the horizon and determine the expectation values ϕ_* and χ_* at that time. Since we are looking at the cases when the curvaton energy density dominates the Universe at the time of its decay, we can compute

the density perturbation from the curvaton component of (10) and the spectral index from (18). The prediction for the tensor-to-scalar ratio r_T is again calculated from (15), but in this case the spectrum of scalar perturbations is given by the second term on the right-hand side of (13):

$$P_\zeta = \frac{f_\sigma^2}{9} \left(\frac{H_*}{\pi \sigma_*} \right)^2 \quad (20)$$

where in the case of curvaton domination f_σ will be very close to 1. This results in the expression

$$r_T = \frac{9}{f_\sigma^2} \frac{2\sigma_*^2}{M_{Pl}^2} \quad (21)$$

for the tensor-to-scalar ratio.

As in the previous Section, we employ a Markov Chain Monte Carlo algorithm to study the predictions of this model for r_T , while fitting the measured values of δ_H and n_s . We find that this model with two inflatons and one curvaton is indeed able to accommodate values of r_T that are in agreement with the Planck results. The left panel of Fig. 5 shows the spectral index and the tensor-to-scalar ratio of this 3-field model, and the model is compared to the Planck data in Fig. 7.

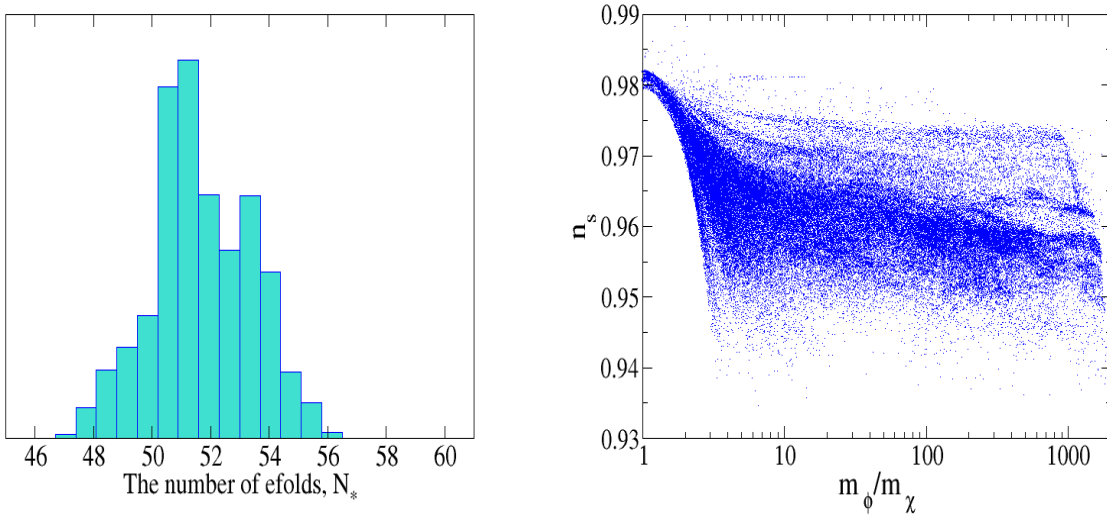


Figure 5: *The left panel shows the number of e-folds in the model with 2 inflatons and a curvaton, which is slightly lower than for the curvaton scenario with a single inflaton. The right panel shows the dependence of the spectral index n_s on the ratio of m_ϕ and m_χ , showing that degenerate situations cannot lead to a low enough spectral index.*

Fig. 5 confirms what we expect from (21), namely that a lower value of r_T can be obtained from a lower curvaton expectation value σ_* . However, we also find that there is a minimum in the prediction for the value of r_T . As the curvaton expectation value becomes smaller, it becomes more difficult for the curvaton to dominate completely the energy density of the Universe at the time of its decay. Eventually, for $\sigma_* \sim 5 \times 10^{15}$ GeV the parameter measuring the significance of the curvaton energy density, f_σ , becomes smaller than 1. We

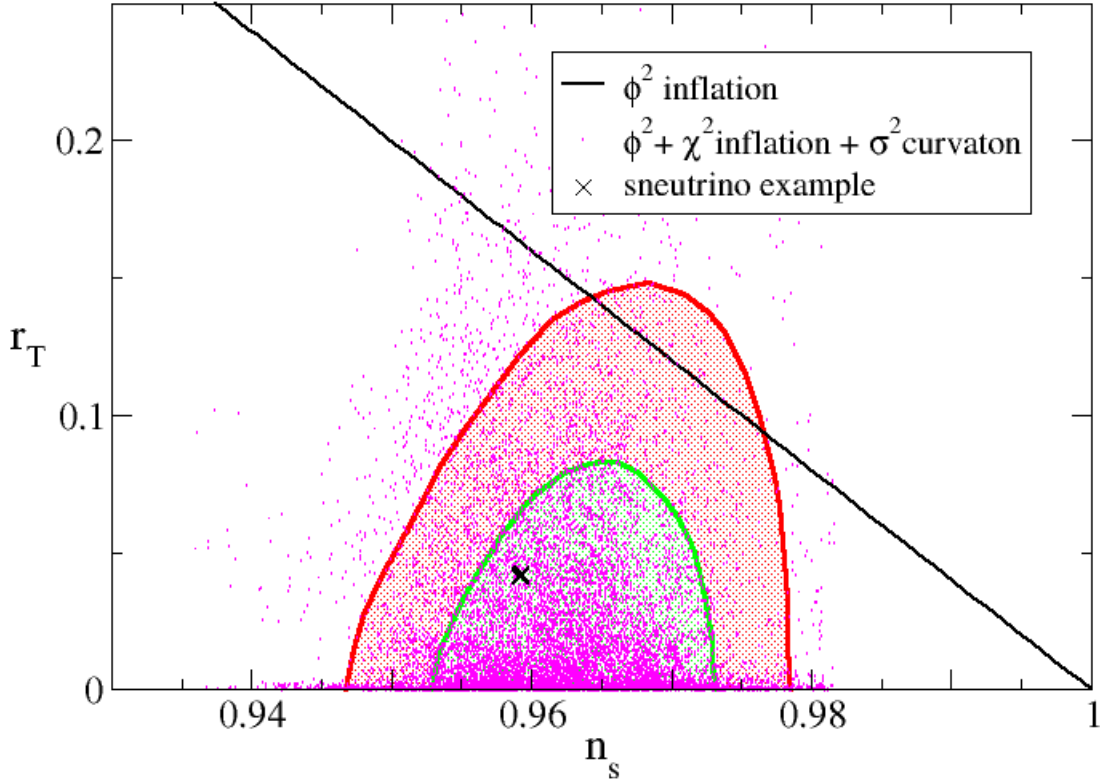


Figure 6: *The model with two inflatons and a curvaton (17) yields good inflationary parameters. Many of the mauve points lie within the region favoured by Planck at the 68% CL. We also show as a black cross a good point in parameter space where the three fields are assumed to be sneutrinos and we also fit the neutrino mass differences and mixings.*

see in Fig. 5 that this corresponds to a minimum value of r_T around 3×10^{-5} . For even smaller curvaton expectation values, the curvaton energy density becomes less significant and f_σ rapidly becomes smaller. This means that the model becomes more and more like the single-field inflation model. In this case we see that the value of r_T begins to grow, as expected. In Fig. 5 we see that the number of efolds N_* is slightly lower than in the case with one inflaton and one curvaton, and that in order to obtain a good spectral index we require m_ϕ to be greater than two or three times m_χ .

It is essential that all the fields in our model decay before nucleosynthesis starts. This requirement places a lower constraint on the temperature T_{reh} of the Universe when the last particle in our model decays into radiation, namely $T_{reh} > 2$ MeV [27]. To this end, we calculate the reheating temperature from the total energy density at the time of the last particle's decay:

$$T_{reh} \sim \rho_{\text{last decay}}^{1/4}. \quad (22)$$

We find that, in order to get good inflationary parameters, we typically find a low reheating temperature, e.g., 10^2 - 10^4 GeV, that resolves the cosmological gravitino problem while still respecting the nucleosynthesis constraint.

Finally, we consider the prediction of this model for the non-Gaussianity parameter f_{NL} . For this model to be consistent with the Planck results, it needs to predict a value in the range $f_{NL} = 2.7 \pm 5.8$. This parameter depends on the sequence of oscillations and decays in the model, and is evaluated at the time of the last decay [26, 28, 29]. In the model with two inflatons and one curvaton, we have seen that the energy density of the heavier inflaton is insignificant from the end of inflation onwards. We also note that for such a model to predict a low value of the tensor-to-scalar ratio that is in agreement with the Planck constraint, the curvaton must dominate the energy density when it decays. Therefore, after the end of inflation, we have the equivalent of a model with one inflaton and one curvaton, with the curvaton energy density being the dominant component of the energy density of the Universe, i.e., $f_\sigma \sim 1$ at the epoch of last decay. It was shown in [26] that models with one inflaton and one curvaton, with both particles contributing to the perturbations, cannot predict a large f_{NL} when the curvaton dominates before its decay. In Fig. 2 of [26] we see that, for the range of curvaton expectation values that we have in our model and for $f_\sigma \sim 1$, the non-Gaussianity parameter is small, $f_{NL} \in [-1, 0]$. So this model with two inflatons and one curvaton is in agreement with the constraint imposed by the Planck data.

5 Three-Sneutrino Inflation

As already mentioned, part of our motivation for studying extended models of quadratic inflation was the possibility of rescuing sneutrino inflation. In most supersymmetric seesaw models for the light neutrino masses, there are three heavy singlet supersymmetric partners of (right-handed) neutrinos², each with a quadratic effective potential. In this Section we investigate the possibility of identifying the inflatons and the curvaton of the previous Section with these sneutrinos. Typical masses of the singlet (right-handed) neutrino fields

²The neutrino oscillation data require only two light neutrinos to have non-zero masses, which is possible in principle with just two heavy singlet neutrinos in a Type-I seesaw model.

are of order 10^8 - 10^{13} GeV, without extreme fine-tuning of the Yukawa couplings³. We look here for models that can explain neutrino masses and mixing angles as well as provide good parameters for Planck observables.

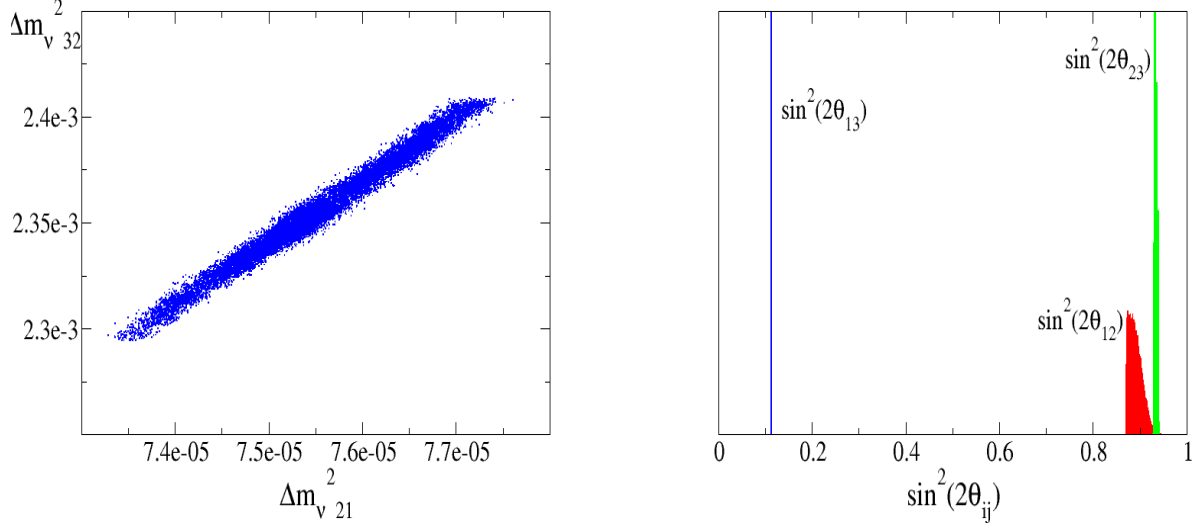


Figure 7: In the left panel we show the mass-squared differences for the neutrino model outlined in the text, and in the right panel we show the three mixing angles. These come from a mass matrix that also yields a good fit to Planck data.

We start with the following mass matrix for the singlet (right-handed) (s)neutrinos⁴:

$$M_\nu = \begin{pmatrix} M_\phi & 0 & 0 \\ 0 & M_\chi & 0 \\ 0 & 0 & M_\sigma \end{pmatrix}, \quad (23)$$

and a 3×3 Yukawa matrix:

$$Y_\nu = \begin{pmatrix} y_{11} & y_{12} & y_{13} \\ y_{21} & y_{22} & y_{23} \\ y_{31} & y_{32} & y_{33} \end{pmatrix}. \quad (24)$$

The decay rate of each heavy particle is then given by [30]

$$\Gamma_i = \frac{1}{8\pi} [Y_\nu^\dagger Y_\nu]_{ii} M_i, \quad (25)$$

where $i = \phi, \chi, \sigma$.

The usual left-handed neutrino mass matrix depends upon the masses and Yukawa couplings of the heavy neutrinos, and is given by:

$$m_\nu = v^2 Y_\nu^\dagger \frac{1}{M_\nu} Y_\nu. \quad (26)$$

³In the Standard Model these range from order unity for the top quark down to order 10^{-6} for the electron, so a wide range of possible values could be considered.

⁴Supersymmetry breaking is not important for our analysis.

By diagonalizing this expression we obtain three eigenvalues, which are the three neutrino masses, and three eigenvectors, which determine the unitary mixing matrix U :

$$\begin{pmatrix} m_{\nu 1} & 0 & 0 \\ 0 & m_{\nu 2} & 0 \\ 0 & 0 & m_{\nu 3} \end{pmatrix} \equiv U^\dagger m_\nu U. \quad (27)$$

Here U is the leptonic equivalent of the CKM matrix in the quark sector [31, 32], which can be written in the following parametrization:

$$U = \begin{pmatrix} c_{12}c_{13} & s_{12}c_{13} & s_{13} \\ -s_{12}c_{23} - c_{12}s_{23}s_{13} & c_{12}c_{23} - s_{12}s_{23}s_{13} & s_{23}c_{13} \\ s_{12}s_{23} - c_{12}c_{23}s_{13} & -c_{12}s_{23} - s_{12}c_{23}s_{13} & c_{23}c_{13} \end{pmatrix}, \quad (28)$$

where $c_{ij} = \cos(\theta_{ij})$ and $s_{ij} = \sin(\theta_{ij})$. This matrix contains three neutrino mixing angles $\theta_{12}, \theta_{23}, \theta_{13}$. In general, the mixing matrix U can also contain CP-violating phases, one detectable in neutrino oscillations and two Majorana phases that would affect neutrinoless double- β decay. For simplicity, here we discard these phases and assume a real Yukawa matrix for the sneutrinos.

We use the 3 masses $m_{\nu i}$ to fit the two measured light-neutrino mass-squared differences $\Delta m_{21}^2 = (7.59 \pm 0.20) \times 10^{-5} eV^2$ and $\Delta m_{32}^2 = (2.43 \pm 0.13) \times 10^{-3} eV^2$. We then choose U to fit the three mixing angles $\sin^2(2\theta_{12}) = 0.87 \pm 0.03$, $\sin^2(2\theta_{23}) > 0.92$ and $\sin^2(2\theta_{13}) = 0.092 \pm 0.021$, as measured in neutrino oscillation experiments [33].

Within this framework, we display one illustrative model with two sneutrino inflatons and one curvaton that leads to predictions for the tensor-to-scalar ratio and the scalar spectral index that are consistent with the Planck results. The parameters of this model are outlined in Table 2, and the corresponding point in parameter space is shown as a black cross in the right panel of Fig. 7.

6 Conclusions

In this paper we have looked for the simplest possible fit to the Planck data using only fields with quadratic potentials. We first recalled the well-known result that single-field quadratic inflation is under pressure from the Planck data. We then went on to show that, while quadratic inflation with a quadratic curvaton fits the data slightly better, it also is disfavoured in its simplest form. This is because the power spectrum is fixed during the normal single-field inflationary phase, and requiring enough efolds forces one to focus on the region where n_s is too high. We went on to show that with three quadratic potentials we can fit both n_s and r_T . We also found that such a model provides a minimum in the prediction for the value of r_T . Finally, we exhibited a model where the three quadratic fields are identified with three sneutrino fields, two playing the rôles of inflatons and one being a curvaton, displaying one example of a point in parameter space that fits both the neutrino and cosmological data.

Our results show that it is possible to rescue quadratic inflation, and that this does not require a very exotic model. Indeed, the three fields required can be identified with singlet (right-handed) sneutrinos.

Parameter	Value
m_ϕ	2.6×10^{12} GeV
Γ_ϕ	2.2×10^8 GeV
ϕ_*	2.2×10^{19} GeV
m_χ	2.2×10^{10} GeV
Γ_χ	1.5×10^4 GeV
χ_*	2.4×10^{19} GeV
m_σ	980 GeV
Γ_σ	1.8×10^{-14} GeV
σ_*	1.2×10^{17} GeV
T_{reheat}	2.7×10^3 GeV
δ_H	1.8×10^{-5}
n_s	0.9592
r_T	0.042
$m_{\nu 1}$	4.85×10^{-2} eV
$m_{\nu 2}$	4.92×10^{-2} eV
$m_{\nu 3}$	3.1×10^{-7} eV
θ_{ij}	see Fig. 6
δm_{ij}^2	see Fig. 6

Table 2: Example of a fit to the Planck and neutrino data. Variations of the parameters around this particular solution of a few % are also compatible with the data, and other solutions may exist.

Acknowledgments

The work of J.E. was supported in part by the London Centre for Terauniverse Studies (LCTS), using funding from the European Research Council via the Advanced Investigator Grant 267352. J.E. and M.F. are grateful for funding from the Science and Technology Facilities Council (STFC).

References

- [1] J. Martin, C. Ringeval and V. Vennin, arXiv:1303.3787 [astro-ph.CO].
- [2] D. Croon, J. Ellis and N. E. Mavromatos, Physics Letters B **724** (2013) , 165 [arXiv:1303.6253 [astro-ph.CO]].
- [3] J. Ellis, D. V. Nanopoulos and K. A. Olive, Phys. Rev. Lett. **111** (2013) 111301 [arXiv:1305.1247 [hep-th]] and JCAP **1310** (2013) 009 [arXiv:1307.3537 [hep-th]].
- [4] K. Nakayama, F. Takahashi and T. T. Yanagida, JCAP **1308** (2013) 038 [arXiv:1305.5099 [hep-ph]] and arXiv:1311.4253 [hep-ph].
- [5] R. Kallosh and A. Linde, JCAP **1306** (2013) 028 [arXiv:1306.3214 [hep-th]]; JCAP **1307** (2013) 002 [arXiv:1306.5220 [hep-th]].
- [6] W. Buchmuller, V. Domcke and K. Kamada, Phys. Lett. B **726** (2013) 467 [arXiv:1306.3471 [hep-th]].
- [7] F. Farakos, A. Kehagias and A. Riotto, Nucl. Phys. B **876** (2013) 187 [arXiv:1307.1137 [hep-th]].
- [8] D. Roest, M. Scalisi and I. Zavala, JCAP **1311** (2013) 007 [arXiv:1307.4343 [hep-th]].
- [9] E. Kiritsis, JCAP **1311** (2013) 011 [arXiv:1307.5873 [hep-th]].
- [10] J. Ellis and N. E. Mavromatos, Phys. Rev. D **88** (2013) 085029 [arXiv:1308.1906 [hep-th]].
- [11] P. Fre and A. S. Sorin, arXiv:1308.2332 [hep-th] and arXiv:1310.5278 [hep-th].
- [12] T. Li, Z. Li and D. V. Nanopoulos, arXiv:1310.3331 [hep-ph] and arXiv:1311.6770 [hep-ph].
- [13] G. Hinshaw *et al.* [WMAP Collaboration], Astrophys. J. Suppl. **208** (2013) 19 [arXiv:1212.5226 [astro-ph.CO]].
- [14] P. A. R. Ade *et al.* [Planck Collaboration], arXiv:1303.5062 [astro-ph.CO].
- [15] P. A. R. Ade *et al.* [Planck Collaboration], arXiv:1303.5082 [astro-ph.CO].
- [16] J. R. Ellis, M. Raidal and T. Yanagida, Phys. Lett. B **581** (2004) 9 [hep-ph/0303242].
- [17] A. R. Liddle, D. Lyth, Cosmological Inflation and Large-Scale Structure, (CAMBRIDGE UNIVERSITY PRESS, 2000)

- [18] C. T. Byrnes and D. Wands, Phys. Rev. D **74** (2006) 043529 [astro-ph/0605679].
- [19] D. Wands, N. Bartolo, S. Matarrese and A. Riotto, Phys. Rev. D **66** (2002) 043520 [astro-ph/0205253].
- [20] A. R. Liddle and D. H. Lyth, Phys. Rept. **231** (1993) 1 [astro-ph/9303019].
- [21] D. H. Lyth, C. Ungarelli and D. Wands, Phys. Rev. D **67** (2003) 023503 [astro-ph/0208055].
- [22] D. H. Lyth and D. Wands, Phys. Lett. B **524** (2002) 5 [hep-ph/0110002].
- [23] K. Dimopoulos, G. Lazarides, D. Lyth and R. Ruiz de Austri, Phys. Rev. D **68** (2003) 123515 [hep-ph/0308015].
- [24] K. Enqvist and T. Takahashi, JCAP **0809** (2008) 012 [arXiv:0807.3069 [astro-ph]].
- [25] J. Fonseca and D. Wands, JCAP **1206** (2012) 028 [arXiv:1204.3443 [astro-ph.CO]].
- [26] M. Sueiro and M. Fairbairn, Phys. Rev. D **87** (2013) 4, 043524 [arXiv:1208.0559 [astro-ph.CO]].
- [27] E. Kolb, M. Turner The Early Universe, (Westview Press, 1994).
- [28] H. Assadullahi, J. Valiviita and D. Wands, Phys. Rev. D **76** (2007) 103003 [arXiv:0708.0223 [hep-ph]].
- [29] D. Langlois, Prog. Theor. Phys. Suppl. **190** (2011) 90 [arXiv:1102.5052 [astro-ph.CO]].
- [30] J. R. Ellis, Nucl. Phys. Proc. Suppl. **137** (2004) 190 [hep-ph/0403247].
- [31] K. Nakamura *et al.* JPG **37**, 075021 (2010).
- [32] W. Rodejohann, Pramana **72** (2009) 217 [arXiv:0804.3925 [hep-ph]].
- [33] C. Cheung, L. J. Hall and D. Pinner, arXiv:1103.3520 [hep-ph].